

## Fe XVIII Emission Lines in Solar X-Ray Spectra

15 January 1998

Prepared by

G. A. WARREN, F. P. KEENAN, and C. J. GREER  
Department of Pure and Applied Physics  
The Queen's University of Belfast, Northern Ireland

K. J. H. PHILLIPS  
Astrophysics Division  
Rutherford Appleton Laboratory  
Oxfordshire, England

M. E. BRUNER and W. A. BROWN  
Lockheed Palo Alto Research Laboratory  
Palo Alto, California

D. L. McKENZIE  
Space and Environment Technology Center  
The Aerospace Corporation  
Los Angeles, California

Prepared for

SPACE AND MISSILE SYSTEMS CENTER  
AIR FORCE MATERIEL COMMAND  
2430 E. El Segundo Boulevard  
Los Angeles Air Force Base, CA 90245

Engineering and Technology Group

APPROVED FOR PUBLIC RELEASE;  
DISTRIBUTION UNLIMITED

19981215 081



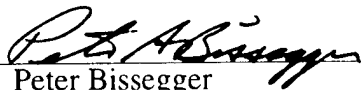
**THE AEROSPACE  
CORPORATION**

El Segundo, California

This report was submitted by The Aerospace Corporation, El Segundo, CA 90245-4691, under Contract No. F04701-93-C-0094 with the Space and Missile Systems Center, 2430 E. El Segundo Blvd., Los Angeles Air Force Base, CA 90245. It was reviewed and approved for The Aerospace Corporation by A. B. Christensen Principal Director, Space and Environment Technology Center. Col. C. Whited was the project officer for the Mission-Oriented Investigation and Experimentation (MOIE) program.

This report has been reviewed by the Public Affairs Office (PAS) and is releasable to the National Technical Information Service (NTIS). At NTIS, it will be available to the general public, including foreign nationals.

This technical report has been reviewed and is approved for publication. Publication of this report does not constitute Air Force approval of the report's findings or conclusions. It is published only for the exchange and stimulation of ideas.

A handwritten signature in dark ink, appearing to read "Peter Bissegger", is written over a horizontal line.

Peter Bissegger  
SMC/AXES

# REPORT DOCUMENTATION PAGE

Form Approved  
OMB No. 0704-0188

Public reporting burden for this collection of information is estimated to average 1 hour per response, including the time for reviewing instructions, searching existing data sources, gathering and maintaining the data needed, and completing and reviewing the collection of information. Send comments regarding this burden estimate or any other aspect of this collection of information, including suggestions for reducing this burden to Washington Headquarters Services, Directorate for Information Operations and Reports, 1215 Jefferson Davis Highway, Suite 1204, Arlington, VA 22202-4302, and to the Office of Management and Budget, Paperwork Reduction Project (0704-0188), Washington, DC 20503.

1. AGENCY USE ONLY (Leave blank)		2. REPORT DATE 15 January 1998		3. REPORT TYPE AND DATES COVERED	
4. TITLE AND SUBTITLE Fe XVIII Emission Lines in Solar X-Ray Spectra				5. FUNDING NUMBERS F04701-93-C-0094	
6. AUTHOR(S) G. A. Warren, F. P. Keenan, C. J. Greer, K. J. H. Phillips, M. E. Bruner, W. A. Brown, and D. L. McKenzie					
7. PERFORMING ORGANIZATION NAME(S) AND ADDRESS(ES) The Aerospace Corporation Technology Operations El Segundo, CA 90245-4691				8. PERFORMING ORGANIZATION REPORT NUMBER TR-96(8570)-4	
9. SPONSORING/MONITORING AGENCY NAME(S) AND ADDRESS(ES) Space and Missile Systems Center Air Force Materiel Command 2430 E. El Segundo Boulevard Los Angeles Air Force Base, CA 90245				10. SPONSORING/MONITORING AGENCY REPORT NUMBER SMC-TR-98-36	
11. SUPPLEMENTARY NOTES					
12a. DISTRIBUTION/AVAILABILITY STATEMENT Approved for public release; distribution unlimited				12b. DISTRIBUTION CODE	
13. ABSTRACT (Maximum 200 words) We have calculated intensity ratios for emission lines of Fe XVIII in the 19–94Å wavelength range at electron temperatures characteristic of the solar corona, $T_e = 2-10 \times 10^6$ K. Our model ion includes data for transitions among the $2s^2 2p^5$ , $2s 2p^6$ , $2s^2 2p^4 3l$ , and $2s 2p^5 3l$ ( $l = s, p$ , and $d$ ) states. Test calculations that omit the $2s^2 2p^5 3l$ levels show that cascades from these are important. We compare our results with observed ratios determined from four solar X-ray instruments, a rocket-borne spectrograph, and spectrometers on the P78-1, OV1-17 and Solar Maximum Mission (SMM) satellites. In addition, we have generated synthetic spectra which we compare directly with flare observations from SMM. Agreement between theory and observation is generally quite good, with differences that are mostly less than 30%, providing limited support for the accuracy of the atomic physics data used in our calculations. However, large discrepancies are found for ratios involving the $2s^2 2p^5 2P_{3/2} - 2s 2p^6 2S$ line at 93.84Å, which currently remain unexplained. Our analysis indicates that the Fe XVIII feature at 15.83Å is the $2s^2 2p^5 2P_{3/2} - 2s^2 2p^4 (3P) 3s^4 P_{3/2}$ transition, rather than $2s^2 2p^5 2P_{3/2} - 2s^2 2p^4 (3P) 3s^2 P_{3/2}$ , as suggested by some authors.					
14. SUBJECT TERMS Solar X-Rays, Solar Corona				15. NUMBER OF PAGES 10	
				16. PRICE CODE	
17. SECURITY CLASSIFICATION OF REPORT UNCLASSIFIED	18. SECURITY CLASSIFICATION OF THIS PAGE UNCLASSIFIED	19. SECURITY CLASSIFICATION OF ABSTRACT UNCLASSIFIED	20. LIMITATION OF ABSTRACT		

## **Acknowledgments**

This work was supported by NATO through travel grant CRG.930722. GAW, FPK, and CJG acknowledge financial support from PPARC, the Royal Society, and the Department of Education (NI), respectively.

## Contents

1. Introduction .....	1
2. Theoretical Ratios and Synthetic Spectra .....	1
3. Observations .....	3
4. Results and Discussion .....	3
4.1 Line Ratios .....	3
4.2 Synthetic Spectra .....	7
5. Conclusions .....	8
References .....	10

## Figures

1. The theoretical Fe XVIII line intensity ratio $R_1$ .....	6
2. The theoretical Fe XVIII line intensity ratio $R_2$ .....	7
3. The Fe XVIII emission line spectrum in the 14.0–14.8 Å wavelength range .....	8
4. The Fe XVIII emission line spectrum in the 15.4–16.2 Å wavelength range .....	9

## Tables

I. Energy levels of $\text{Fe}^{+17}$ .....	2
II. Observed and theoretical Fe XVIII line ratios .....	4

## 1. Introduction

Emission lines of iron ions feature strongly in astrophysical spectra, due to the high cosmic abundance of this element. In particular, the soft X-ray spectrum (10–100 Å) of the solar corona is dominated by the emission lines of highly ionized iron ions from Fe XIV to Fe XIX. Solar flares and active regions have often been observed in this wavelength region (Neupert *et al.*, 1967; Parkinson, 1975; Rugge and Walker, 1978; McKenzie *et al.*, 1980; Phillips *et al.*, 1982; Acton *et al.*, 1985), and lines of Fe XVIII are commonly detected, which in general have been firmly identified (Feldman *et al.*, 1973).

Under coronal conditions, line ratios in Fe XVIII should be relatively electron density insensitive, and hence a function of electron temperature  $T_e$  only. In particular, lines with a large wavelength separation should give very sensitive diagnostic ratios for  $T_e$  (Keenan, 1992). Here we present calculations of the Fe XVIII emission line spectrum in the soft X-ray wavelength range, and compare these with solar observational data from a variety of sources, to investigate both the accuracy of the theoretical results and their usefulness as electron temperature diagnostics.

## 2. Theoretical Ratios and Synthetic Spectra

The model ion for Fe XVIII consisted of the 108 fine-structure levels in the  $2s^22p^5$ ,  $2s2p^6$ ,  $2s^22p^43l$ , and  $2s2p^53l$  ( $l = s, p$ , and  $d$ ) terms, the energies of which were taken from Cornille *et al.* (1992). We have also adopted the level-numbering scheme of these authors, which is given in Table I. Electron impact excitation rates were taken where available from the **R**-matrix calculations of Mohan *et al.* (1987) and Saraph and Tully (1994), the SUPERSTRUCTURE results of Cornille *et al.* being adopted for other transitions. Einstein A-coefficients were obtained from Cornille *et al.* and Blackford and Hibbert (1994). Proton impact excitation rates, which are only important for the  $2s^22p^5\ ^2P_{3/2} - 2s^22p^5\ ^2P_{1/2}$  transition (Seaton, 1964), were taken from Foster, Keenan, and Reid (1994).

We have used the above atomic data in conjunction with the statistical equilibrium code of Dufton (1977) to calculate relative level populations, and hence line intensity ratios, for a temperature range over which Fe XVIII ions are abundant in a collisionally ionized plasma (Arnaud and Raymond, 1992). Details of the procedures involved and approximations made in the calculations may be found in Dufton (1977) and Dufton *et al.* (1978). Given that the adopted atomic data should be accurate to approximately  $\pm 10\%$  in most instances (see references above), we believe that the resultant theoretical line ratios should therefore be reliable to better than  $\pm 20\%$ .

Table I  
Energy levels of Fe<sup>+17</sup>

Level	Index	Level	Index	Level	Index
$1s^2 2s^2 2p^5$	$^2P_{3/2}$ 1	$2s^2 2p^4(^3P)3d$	$^4P_{1/2}$ 37	$2s2p^5(^3P)3p$	$^2D_{5/2}$ 73
$2s^2 2p^5$	$^2P_{1/2}$ 2	$2s^2 2p^4(^1S)3p$	$^2P_{3/2}$ 38	$2s2p^5(^3P)3p$	$^2P_{1/2}$ 74
$2s2p^6$	$^2S_{1/2}$ 3	$2s^2 2p^4(^3P)3d$	$^4P_{3/2}$ 39	$2s2p^5(^3P)3p$	$^4P_{3/2}$ 75
$2s^2 2p^4(^3P)3s$	$^4P_{5/2}$ 4	$2s^2 2p^4(^1S)3p$	$^4P_{3/2}$ 40	$2s2p^5(^3P)3p$	$^4P_{1/2}$ 76
$2s^2 2p^4(^3P)3s$	$^2P_{3/2}$ 5	$2s^2 2p^4(^3P)3d$	$^2F_{5/2}$ 41	$2s2p^5(^1P)3s$	$^2P_{3/2}$ 77
$2s^2 2p^4(^3P)3S$	$^4P_{1/2}$ 6	$2s^2 2p^4(^3P)3d$	$2P_{1/2}$ 42	$2s2p^5(^1P)3s$	$^2P_{1/2}$ 78
$2s^2 2p^4(^3P)3s$	$^4P_{3/2}$ 7	$2s^2 2p^4(^3P)3d$	$^4F_{3/2}$ 43	$2s2p^5(^3P)3p$	$^2D_{3/2}$ 79
$2s^2 2p^4(^3P)3s$	$^2P_{1/2}$ 8	$2s^2 2p^4(^3P)3d$	$^4F_{5/2}$ 44	$2s2p^5(^3P)3p$	$^2S_{1/2}$ 80
$2s^2 2p^4(^1D)3s$	$^2D_{5/2}$ 9	$2s^2 2p^4(^3P)3d$	$^4F_{7/2}$ 45	$2s2p^5(^3P)3d$	$^4P_{1/2}$ 81
$2s^2 2p^4(^1D)3s$	$^2D_{3/2}$ 10	$2s^2 2p^4(^3P)3d$	$^2D_{3/2}$ 46	$2s2p^5(^3P)3d$	$^4P_{3/2}$ 82
$2s^2 2p^4(^3P)3p$	$^4P_{3/2}$ 11	$2s^2 2p^4(^3P)3d$	$^4P_{5/2}$ 47	$2s2p^5(^3P)3d$	$^4F_{9/2}$ 83
$2s^2 2p^4(^3P)3p$	$^4P_{5/2}$ 12	$2s^2 2p^4(^3P)3d$	$^2P_{3/2}$ 48	$2s2p^5(^3P)3d$	$^4P_{5/2}$ 84
$2s^2 2p^4(^3P)3p$	$^4P_{1/2}$ 13	$2s^2 2p^4(^3P)3d$	$^2D_{5/2}$ 49	$2s2p^5(^3P)3d$	$^4F_{7/2}$ 85
$2s^2 2p^4(^3P)3p$	$^4D_{7/2}$ 14	$2s^2 2p^4(^1D)3d$	$^2G_{7/2}$ 50	$2s2p^5(^3P)3d$	$^4F_{5/2}$ 86
$2s^2 2p^4(^3P)3p$	$^2D_{5/2}$ 15	$2s^2 2p^4(^1D)3d$	$^2G_{9/2}$ 51	$2s2p^5(^1P)3p$	$^2D_{3/2}$ 87
$2s^2 2p^4(^3P)3p$	$^2P_{1/2}$ 16	$2s^2 2p^4(^1D)3d$	$^2F_{5/2}$ 52	$2s2p^5(^3P)3d$	$^4D_{7/2}$ 88
$2s^2 2p^4(^3P)3p$	$^4D_{3/2}$ 17	$2s^2 2p^4(^1D)3d$	$^2S_{1/2}$ 53	$2s2p^5(^3P)3d$	$^4F_{3/2}$ 89
$2s^2 2p^4(^3P)3p$	$^4D_{1/2}$ 18	$2s^2 2p^4(^1D)3d$	$^2F_{7/2}$ 54	$2s2p^5(^1P)3p$	$^2F_{7/2}$ 90
$2s^2 2p^4(^3P)3p$	$^2P_{3/2}$ 19	$2s^2 2p^4(^1D)3d$	$^2P_{3/2}$ 55	$2s2p^5(^1P)3p$	$^2P_{1/2}$ 91
$2s^2 2p^4(^1S)3S$	$^2S_{1/2}$ 20	$2s^2 2p^4(^1D)3d$	$^2D_{5/2}$ 56	$2s2p^5(^1P)3p$	$^2P_{3/2}$ 92
$2s^2 2p^4(^3P)3p$	$^4D_{5/2}$ 21	$2s^2 2p^4(^1D)3d$	$^2D_{3/2}$ 57	$2s2p^5(^3P)3d$	$^4D_{1/2}$ 93
$2s^2 2p^4(^3P)3p$	$^4S_{3/2}$ 22	$2s^2 2p^4(^1D)3d$	$^2P_{1/2}$ 58	$2s2p^5(^3P)3d$	$^2D_{5/2}$ 94
$2s^2 2p^4(^3P)3p$	$^4S_{1/2}$ 23	$2s2p^5(^3P)3s$	$^4P_{5/2}$ 59	$2s2p^5(^3P)3d$	$^4D_{5/2}$ 95
$2s^2 2p^4(^3P)3p$	$^2D_{3/2}$ 24	$2s^2 2p^4(^1S)3d$	$^2D_{5/2}$ 60	$2s2p^5(^3P)3d$	$^2F_{7/2}$ 96
$2s^2 2p^4(^1D)3p$	$^2F_{5/2}$ 25	$2s2p^5(^3P)3s$	$^4P_{3/2}$ 61	$2s2p^5(^3P)3d$	$^4D_{3/2}$ 97
$2s^2 2p^4(^1D)3p$	$^2F_{7/2}$ 26	$2s2p^5(^1S)3d$	$^2D_{3/2}$ 62	$2s2p^5(^3P)3d$	$^2D_{3/2}$ 98
$2s^2 2p^4(^1D)3p$	$^2D_{3/2}$ 27	$2s2p^5(^3P)3s$	$^4P_{1/2}$ 63	$2s2p^5(^1P)3p$	$^2S_{1/2}$ 99
$2s^2 2p^4(^1D)3p$	$^2D_{5/2}$ 28	$2s2p^5(^3P)3s$	$^2P_{3/2}$ 64	$2s2p^5(^3P)3d$	$^2P_{1/2}$ 100
$2s^2 2p^4(^1D)3p$	$^2P_{3/2}$ 29	$2s2p^5(^3P)3s$	$^2P_{1/2}$ 65	$2s2p^5(^3P)3d$	$^2F_{5/2}$ 101
$2s^2 2p^4(^1D)3p$	$^2P_{1/2}$ 30	$2s2p^5(^3P)3p$	$^4S_{3/2}$ 66	$2s2p^5(^3P)3d$	$^2P_{3/2}$ 102
$2s^2 2p^4(^3P)3d$	$^4D_{5/2}$ 31	$2s2p^5(^3P)3p$	$^4D_{5/2}$ 67	$2s2p^5(^1P)3d$	$^2F_{5/2}$ 103
$2s^2 2p^4(^3P)3d$	$^4D_{7/2}$ 32	$2s2p^5(^3P)3p$	$^4D_{7/2}$ 68	$2s2p^5(^1P)3d$	$^2F_{7/2}$ 104
$2s^2 2p^4(^3P)3d$	$^4D_{3/2}$ 33	$2s2p^5(^3P)3p$	$^4D_{3/2}$ 69	$2s2p^5(^1P)3d$	$^2P_{3/2}$ 105
$2s^2 2p^4(^3P)3d$	$^4D_{1/2}$ 34	$2s2p^5(^3P)3p$	$^4P_{5/2}$ 70	$2s2p^5(^1P)3d$	$^2D_{5/2}$ 106
$2s^2 2p^4(^3P)3d$	$^4F_{9/2}$ 35	$2s2p^5(^3P)3p$	$^4D_{1/2}$ 71	$2s2p^5(^1P)3d$	$^2D_{3/2}$ 107
$2s^2 2p^4(^3P)3d$	$^2F_{7/2}$ 36	$2s2p^5(^3P)3p$	$^2P_{3/2}$ 72	$2s2p^5(^1P)3d$	$^2P_{1/2}$ 108

If we take account of the dominant line-broadening mechanisms, including Doppler and instrumental, we may generate synthetic line spectra from the results of the line ratio calculations. Here we have used the procedures discussed in detail by Phillips *et al.* (1993) to construct a sequence of theoretical Fe XVIII spectra at selected temperatures, for comparison with observed spectral data.

### 3. Observations

We compare our calculated line ratios and synthetic spectra with four sets of X-ray solar observations, which are briefly described below. Details of the instrumentation employed may be found in the references listed.

(1) Acton *et al.* (1985). This spectrum, covering 10–100 Å with a resolution of 20 mÅ, is of an M-class solar flare observed on 1982 July 13 by a rocket-borne 5 m grazing-incidence spectrograph.

(2) McKenzie *et al.* (1992). These data, of a composite active region spectrum, were obtained by the SOLEX B crystal spectrometer on the US Department of Defense P78–1 satellite during 1979. They cover the wavelength range 8–23 Å, with a spectral resolution of 30 mÅ.

(3) Rugge and Walker (1978). These line ratios are from data taken by a crystal spectrometer on the OV1–17 satellite on 1969 March 20–21, under various conditions of the solar corona, in the wavelength range 1.5–25 Å, and with a spectral resolution of  $\sim 10$  mÅ.

(4) Solar Maximum Mission (SMM) satellite. In this case we also compare our calculations directly with the spectra via spectral synthesis. The observations are of an active region, obtained by the Flat Crystal Spectrometer on board SMM on 1986 October 19. This instrument covered the wavelength range from 1.4–22 Å, with a spectral resolution of 13 mÅ in the region of the Fe XVIII lines discussed here (Acton *et al.*, 1980; Phillips *et al.*, 1982).

We note that the Acton *et al.* (1985) spectrum observed not only the  $2s^2 2p^5 - 2s^2 2p^4 3l$  transitions around 13–16 Å detected by the other instruments, but also the  $2s^2 2p^5 \ ^2P_{3/2} - 2s^2 2p^6 \ ^2S$  feature at 93.84 Å. Under coronal conditions, a very sensitive temperature diagnostic is provided by the ratio of this line to shorter-wavelength features.

### 4. Results and Discussion

#### 4.1. LINE RATIOS

In Table II we list ratios involving selected strong, unblended emission lines of Fe XVIII for each of the observational data sources listed in Section 3. For such



Table II  
Observed and theoretical Fe XVIII line ratios

$\lambda$ (Å)	Transition <sup>a</sup>	Observed <sup>b</sup>				Theory <sup>b</sup>		
		Acton	McKenzie	Rugge and	SMM	$\log T_e =$		
		<i>et al.</i> (1985)	<i>et al.</i> (1992)	Walker (1978)	data <sup>c</sup>	6.4	6.7	7.0
13.89	1–60	0.08	–	0.17	–	0.12	0.16	0.23
14.12	1–57	0.10	–	0.09	0.15	0.05	0.06	0.09
14.17	1–56	0.80	1.16	0.87	1.48	1.57	2.06	2.89
14.23	1–53	0.35	0.31	0.31	0.50	0.33	0.43	0.59
14.31	2–58	0.19	–	–	0.09	0.11	0.14	0.20
14.35	1–49	0.40	0.45	–	0.56	0.55	0.68	0.93
14.57	1–37	–	0.08	0.11	0.09	0.10	0.12	0.15
15.42	2–20	0.05	–	–	0.14	0.06	0.06	0.08
15.61	1–9	0.40	0.46	0.41	0.50	0.51	0.58	0.68
15.83	1–5 <sup>d</sup>	0.26	0.34	0.30	0.35	0.51	0.52	0.58
15.83	1–7 <sup>e</sup>	0.26	0.34	0.30	0.35	0.29	0.31	0.36
16.06	1–4	1.00	1.00	1.00	1.00	1.00	1.00	1.00
93.84	1–3	1.47	–	–	–	70.2	18.1	11.8

<sup>a</sup> Level numbering from Table I.

<sup>b</sup> Line intensities normalized to  $I(16.06 \text{ Å}) = 1.00$ , where  $I$  is in photon units.

<sup>c</sup> This paper.

<sup>d</sup> The 15.83 Å line is identified as transition 1–5 ( $2s^2 2p^5 \text{ } ^2P_{3/2} - 2s^2 2p^4 ({}^3P) 3s \text{ } ^2P_{3/2}$ ) by Rugge and Walker (1978), Phillips *et al.* (1982), and McKenzie *et al.* (1992).

<sup>e</sup> The 15.83 Å line is identified as transition 1–7 ( $2s^2 2p^5 \text{ } ^2P_{3/2} - 2s^2 2p^4 ({}^3P) 3s \text{ } ^4P_{3/2}$ ) by Acton *et al.* (1985) and Cornille *et al.* (1992).

strong lines, the line intensities should be accurate to approximately  $\pm 20\%$  (see references in Section 3), and hence the line ratios to better than  $\pm 30\%$ . We note that the ratios for the Acton *et al.* (1985) spectrum are somewhat different from the published values, due to a recent revision of the instrument sensitivity function in first order. Also included in Table II are the corresponding theoretical ratios at three electron temperatures, namely  $\log T_e = 6.4$ , 6.7 and 7.0, i.e., near the temperature ( $T_m$ ) of maximum Fe XVIII abundance in ionization equilibrium, where  $\log T_m = 6.8$  (Arnaud and Raymond, 1992).

Our calculations show that the 93.84 Å line is indeed extremely sensitive to  $T_e$ , in conjunction with the short-wavelength transitions. However, the observed ratio from Acton *et al.* (1985) in Table II differs in all cases by large factors (typically 10) from the theoretical values. It is unlikely that this discrepancy is due to errors in the adopted atomic data, as we find excellent agreement between

theory and experiment for ratios involving the 93.84 Å transition and the Fe XVIII  $2s^2 2p^5 \ ^2P_{3/2} - 2s^2 2p^5 \ ^2P_{1/2}$  forbidden line at 974.8 Å, observed in the JIPP T-II-U tokamak, for which the temperature and density have been independently determined (Foster *et al.*, 1994). In addition, errors in the instrument calibration are unlikely to be responsible for the discrepancies, as the calibration is believed to be accurate to  $\pm 50\%$  over the complete wavelength coverage (Brown, unpublished data). If the 93.84 Å line were blended with nearby features, this would make the disagreement between theory and observation even worse, while although optical depth effects in the line could explain the discrepancy, our calculations indicate that it is optically thin. Clearly, further theoretical and experimental work on the 93.84 Å line, and its intensity relative to the shorter wavelength Fe XVIII features, is urgently required.

As we cannot at present employ the 93.84 Å line for diagnostic purposes, we have used the 1–4 transition ( $2s^2 2p^5 \ ^2P_{3/2} - 2s^2 2p^4(^3P)3s \ ^4P_{5/2}$ ) at 16.06 Å as a reference line. Since it is close in wavelength to the other lines, we expect the resulting ratios to be much less sensitive to variations in the electron temperature, but probably also less susceptible to possible instrument calibration errors. That the temperature sensitivity is indeed diminished can be seen in Table II, where we list computed line ratios for the temperatures indicated above.

From Table II we see that the observed ratios are generally in quite good agreement with the computed ones, differing by an average of  $\sim 30\%$  only from the theoretical values at  $\log T_e = 6.7$ . This provides limited support for the validity of the atomic data and furthermore indicates that the model ion is complete; the effect of cascades from the higher lying  $2p^4 4l$  levels is unimportant, and do not need to be included. We have also estimated the effect of excluding the  $2s 2p^5 3l$  levels, by repeating our calculations using a model ion which includes only the levels 1 to 62 in Table I. This changed all the theoretical ratios by at least 20%. As an illustration, we plot in Figures 1 and 2 the ratios

$$R_1 = I(1 - 53)/I(1 - 4) = I(14.23 \text{ Å})/I(16.06 \text{ Å})$$

and

$$R_2 = I(1 - 49)/I(1 - 4) = I(14.35 \text{ Å})/I(16.06 \text{ Å})$$

calculated with both model ions. We see that excluding the  $2s 2p^5 3l$  levels increases the  $R_1$  ratio by 27%, 44%, and 63% at  $\log T_e = 6.4$ , 6.7, and 7.0, respectively, with the corresponding changes in  $R_2$  being 26%, 43%, and 65%. In all cases this increases the discrepancy with observation.

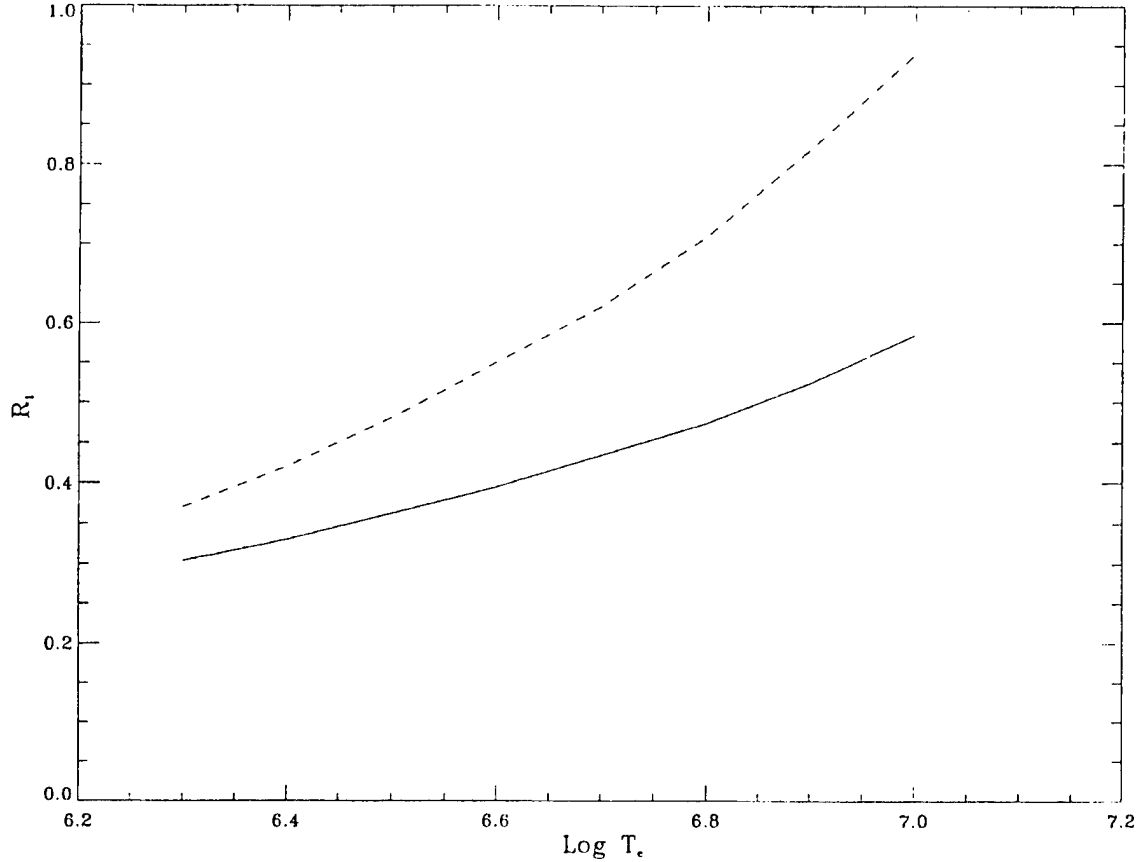


Figure 1. The theoretical Fe XVIII line intensity ratio

$$R_1 = I(2s^2 2p^5 \ ^2P_{3/2} - 2s^2 2p^4 ({}^1D) 3d \ ^2S) / I(2s^2 2p^5 \ ^2P_{3/2} - 2s^2 2p^4 ({}^3P) 3s \ ^4P_{5/2}) \\ = I(14.23 \text{ \AA}) / I(16.06 \text{ \AA}),$$

where  $I$  is in photon units, plotted as a function of electron temperature. The solid line shows the ratios calculated when the  $2s2p^5 3l$  levels are included in the model ion, while the dashed line shows the effects of excluding these levels.

The identity of the Fe XVIII line at 15.83 Å is uncertain. Rugge and Walker (1978), Phillips *et al.* (1982), and McKenzie *et al.* (1992), identify the line with transition 1–5 ( $2s^2 2p^5 \ ^2P_{3/2} - 2s^2 2p^4 ({}^3P) 3s \ ^2P_{3/2}$ ). However, Acton *et al.* (1985) and Cornille *et al.* (1992) identify the line as transition 1–7 ( $2s^2 2p^5 \ ^2P_{3/2} - 2s^2 2p^4 ({}^3P) 3s \ ^4P_{3/2}$ ). To investigate this, in Table II we compare the measured 15.83 Å/16.06 Å line ratios with the theoretical predictions for both the 1–5 and 1–7 identifications. We see that the agreement between theory and observation is much better if the 15.83 Å line is the 1–7 transition, providing support for the identification made by Acton *et al.* and Cornille *et al.*

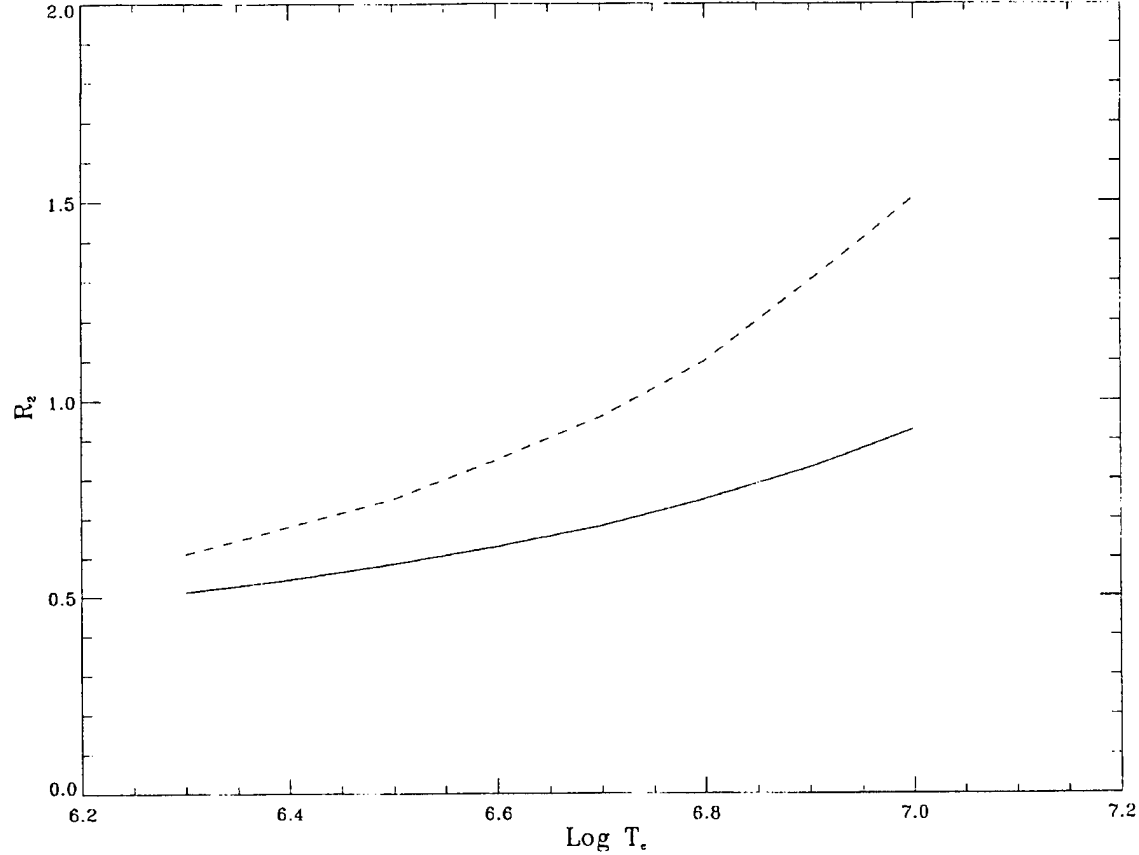


Figure 2. The theoretical Fe XVIII line intensity ratio

$$R_2 = I(2s^2 2p^5 \ ^2P_{3/2} - 2s^2 2p^4 ({}^3P) 3d \ ^2D_{5/2}) / I(2s^2 2p^5 \ ^2P_{3/2} - 2s^2 2p^4 ({}^3P) 3s \ ^4P_{5/2}) \\ = I(14.35 \text{ \AA}) / I(16.06 \text{ \AA}),$$

where  $I$  is in photon units, plotted as a function of electron temperature. The solid line shows the ratios calculated when the  $2s2p^5 3l$  levels are included in the model ion, while the dashed line shows the effects of excluding these levels.

#### 4.2. SYNTHETIC SPECTRA

We have calculated synthetic spectra for several temperatures in the range  $6.4 < \log T_e < 7.0$ , and find the best agreement towards the lower end of the temperature range. Accordingly, in Figures 3 and 4 we plot the observed data together with our theoretical spectra at  $\log T_e = 6.4$ , over the wavelength ranges  $14.0\text{--}14.8 \text{ \AA}$  (which covers the transitions from the  $2s^2 2p^4 3d$  levels), and  $15.4\text{--}16.2 \text{ \AA}$  (transitions from  $2s^2 2p^4 3s$  levels), respectively. For purposes of comparison we have again normalized each spectrum to the intensity of the  $16.06 \text{ \AA}$  line. A few transitions from other ionic species are present in the observed spectrum, including Fe XIX at  $14.67 \text{ \AA}$ , Fe XVII at  $15.45 \text{ \AA}$  and O VIII at  $16.00 \text{ \AA}$  (Phillips *et al.*, 1982), the

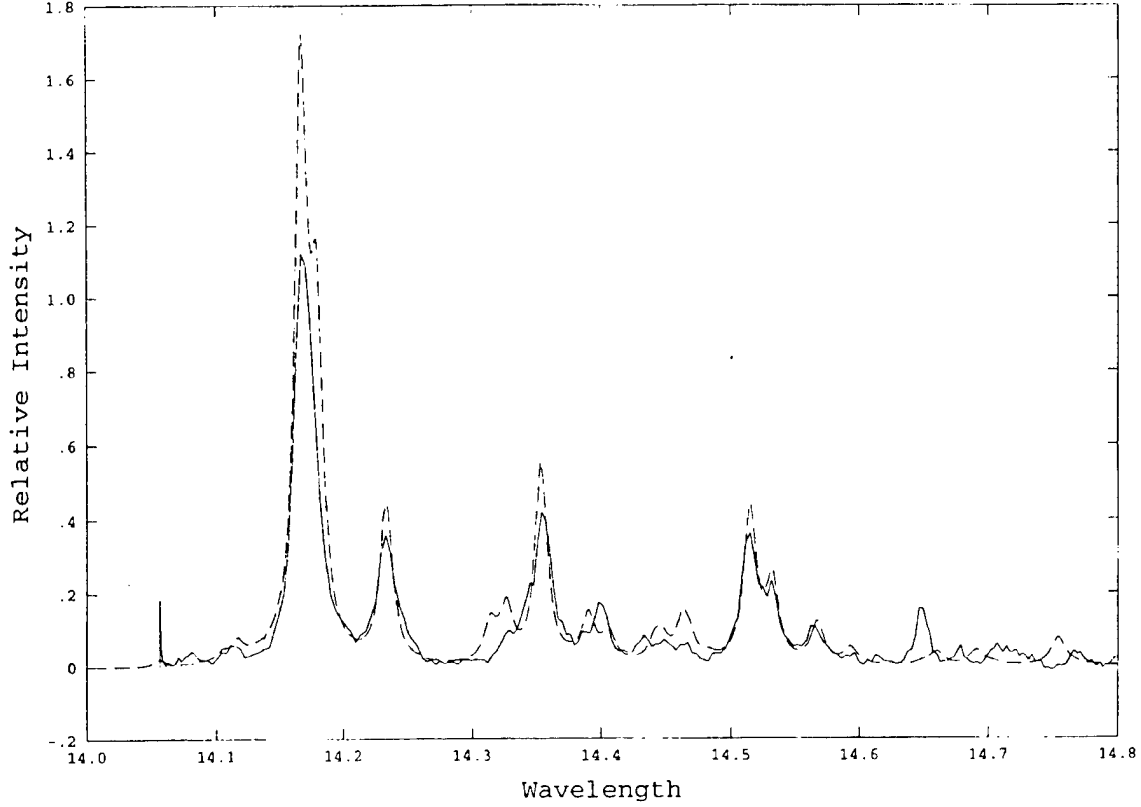


Figure 3. The Fe XVIII emission line spectrum in the 14.0–14.8 Å wavelength range, where the relative intensity is in photon units, with: observed SMM active region data (—); theoretical spectrum at  $\log T_e = 6.4$  (---).

last of which is strongly blended with the Fe XVIII lines 1–5 ( $2s^22p^5\ ^2P_{3/2} - 2s^22p^4(^3P)3s\ ^2P_{3/2}$ ) and 2–8 ( $2s^22p^5\ ^2P_{1/2} - 2s^22p^4(^3P)3s\ ^2P_{1/2}$ ), assuming the identifications of Acton *et al.* (1985) and Cornille *et al.* (1992) are correct. For strong, unblended lines we see that at this temperature the observed and computed peak theoretical intensities are in moderately good agreement, with differences that are mostly less than 30%, providing some limited additional support for the accuracy of the adopted atomic data.

## 5. Conclusions

The  $2s^22p^5\ ^2P_{3/2} - 2s2p^6\ ^2S$  transition in Fe XVIII at 93.84 Å should, in principle, be a very useful reference line for temperature diagnostics in the Sun, since in conjunction with the lines at 13–16 Å it gives very sensitive ratios. However, to exploit this we need further observations and calculations for the Fe XVIII features

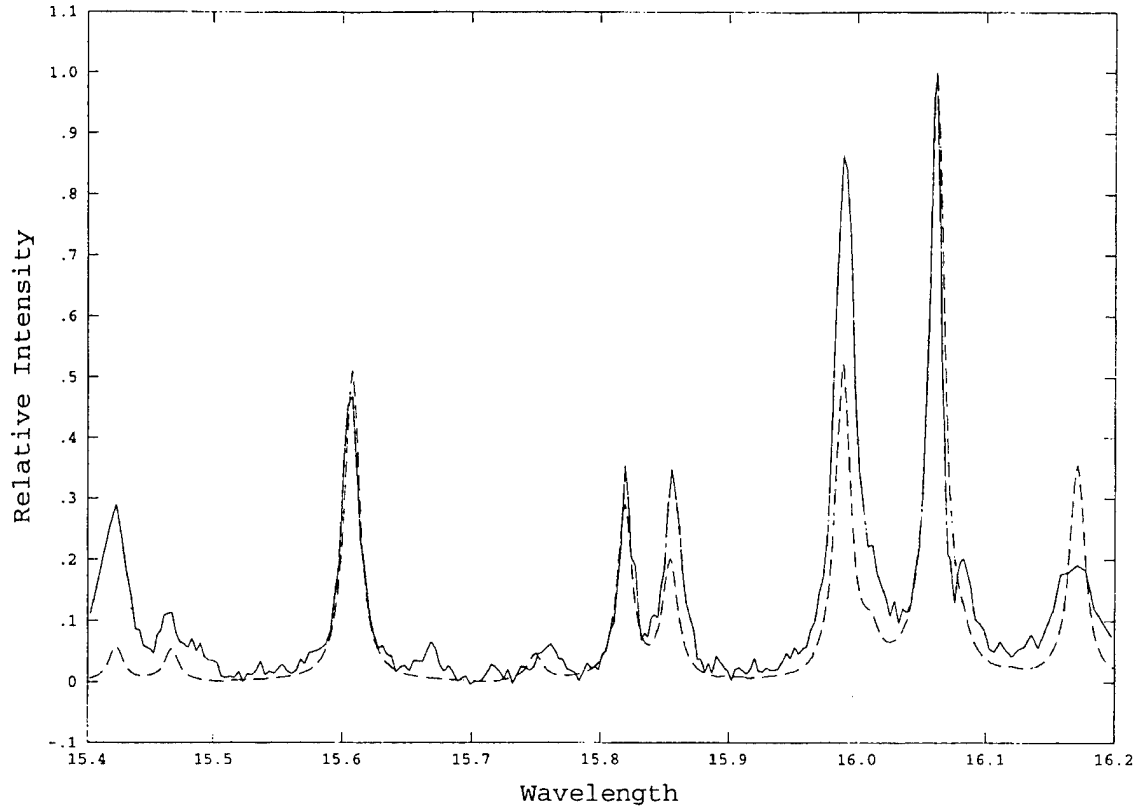


Figure 4. The Fe XVIII emission line spectrum in the 15.4–16.2 Å wavelength range, where the relative intensity is in photon units, with: observed SMM active region data (—); theoretical spectrum at  $\log T_e = 6.4$  (---).

spanning the 10–100 Å wavelength range, since the current agreement between computation and observation is poor.

For lines in the 13–16 Å wavelength interval, agreement between theory and observation (from both line ratio analyses and spectral synthesis) is acceptable, with discrepancies that are generally less than 30%, providing support for the atomic data adopted in the analysis. The presence of the  $2s2p^53l$  levels in the model ion has a significant effect on the calculated line intensity ratios, showing that these levels must be included. A comparison of theoretical results with observed line ratios involving the 15.83 Å feature indicates that this transition is  $2s^22p^5\ ^2P_{3/2} - 2s^22p^4(^3P)3s\ ^4P_{3/2}$ , rather than  $2s^22p^5\ ^2P_{3/2} - 2s^22p^4(^3P)3s\ ^2P_{3/2}$ , as suggested by some authors.

Finally, we note that some of the short wavelength line ratios show a significant variation with electron temperature. For example,  $R_1 = I(14.23\text{ Å})/I(16.06\text{ Å})$  changes by 80% over the temperature interval  $\log T_e = 6.4 - 7.0$  (see Figure 1), while  $R_2 = I(14.35\text{ Å})/I(16.06\text{ Å})$  varies by 70% over the same  $T_e$  range. In the absence of reliable results for the 93.84 Å line, these should be therefore used as  $T_e$ -diagnostics.

## References

- Acton, L. W., Culhane, J. L., Gabriel, A. H., and 21 co-authors: 1980, *Solar Phys.* **65**, 53.
- Acton, L. W., Bruner, M. E., Brown, W. A., Fawcett, B. C., Schweizer, W., and Speer, R. J.: 1985, *Astrophys. J.* **291**, 865.
- Arnaud, M. and Raymond, J.: 1992, *Astrophys. J.* **398**, 394.
- Blackford, H. M. S. and Hibbert, A.: 1994, *Atomic Data Nucl. Data Tables* **58**, 101.
- Cornille, M., Dubau, J., Loulergue, M., Bely-Dubau, F., and Faucher, P.: 1992, *Astron. Astrophys.* **259**, 669.
- Dufton, P. L.: 1977, *Comp. Phys. Comm.* **13**, 25.
- Dufton, P. L., Berrington, K. A., Burke, P. G., and Kingston, A. E.: 1978, *Astron. Astrophys.* **62**, 111.
- Feldman, U., Doschek, G. A., Cowan, R. D., and Cohen, L.: 1973, *J. Opt. Soc. Am.* **63**, 1445.
- Foster, V. J., Keenan, F. P., and Reid, R. H. G.: 1994, *Phys. Rev.* **A49**, 3092.
- Keenan, F. P.: 1992, *Newsletter on Analysis of Astronomical Spectra* **17**, 9.
- McKenzie, D. L., Keenan, F. P., McCann, S. M., Berrington, K. A., Hibbert, A., and Mohan, M.: 1992, *Astrophys. J.* **385**, 378.
- McKenzie, D. L., Landecker, P. B., Broussard, R. M., Rugge, H. R., Young, R. M., Feldman, U., and Doschek, G. A.: 1980, *Astrophys. J.* **241**, 409.
- Mohan, M., Baluja, K. L., Hibbert, A., and Berrington, K. A.: 1987, *J. Phys.* **B20**, 6319.
- Neupert, W. M., Gates, W., Swartz, M., and Young, R.: 1967, *Astrophys. J.* **149**, L79.
- Parkinson, J. H.: 1975, *Solar Phys.* **42**, 183.
- Phillips, K. J. H. *et al.*: 1982, *Astrophys. J.* **256**, 774.
- Phillips, K. J. H., Harra, L. K., Keenan, F. P., Zarro, D. M., and Wilson, M.: 1993, *Astrophys. J.* **419**, 426.
- Rugge, H. R. and Walker, A. B. C.: 1978, *Astrophys. J.* **219**, 1068.
- Saraph, H. E. and Tully, J. A.: 1994, *Astron. Astrophys. Suppl.* **107**, 29.
- Seaton, M. J.: 1964, *Monthly Notices Roy. Astron. Soc.* **127**, 191.

## TECHNOLOGY OPERATIONS

The Aerospace Corporation functions as an "architect-engineer" for national security programs, specializing in advanced military space systems. The Corporation's Technology Operations supports the effective and timely development and operation of national security systems through scientific research and the application of advanced technology. Vital to the success of the Corporation is the technical staff's wide-ranging expertise and its ability to stay abreast of new technological developments and program support issues associated with rapidly evolving space systems. Contributing capabilities are provided by these individual Technology Centers:

**Electronics Technology Center:** Microelectronics, VLSI reliability, failure analysis, solid-state device physics, compound semiconductors, radiation effects, infrared and CCD detector devices, Micro-Electro-Mechanical Systems (MEMS), and data storage and display technologies; lasers and electro-optics, solid state laser design, micro-optics, optical communications, and fiber optic sensors; atomic frequency standards, applied laser spectroscopy, laser chemistry, atmospheric propagation and beam control, LIDAR/LADAR remote sensing; solar cell and array testing and evaluation, battery electrochemistry, battery testing and evaluation.

**Mechanics and Materials Technology Center:** Evaluation and characterization of new materials: metals, alloys, ceramics, polymers and composites; development and analysis of advanced materials processing and deposition techniques; nondestructive evaluation, component failure analysis and reliability; fracture mechanics and stress corrosion; analysis and evaluation of materials at cryogenic and elevated temperatures; launch vehicle fluid mechanics, heat transfer and flight dynamics; aerothermodynamics; chemical and electric propulsion; environmental chemistry; combustion processes; spacecraft structural mechanics, space environment effects on materials, hardening and vulnerability assessment; contamination, thermal and structural control; lubrication and surface phenomena; microengineering technology and microinstrument development.

**Space and Environment Technology Center:** Magnetospheric, auroral and cosmic ray physics, wave-particle interactions, magnetospheric plasma waves; atmospheric and ionospheric physics, density and composition of the upper atmosphere, remote sensing, hyperspectral imagery; solar physics, infrared astronomy, infrared signature analysis; effects of solar activity, magnetic storms and nuclear explosions on the earth's atmosphere, ionosphere and magnetosphere; effects of electromagnetic and particulate radiations on space systems; component testing, space instrumentation; environmental monitoring, trace detection; atmospheric chemical reactions, atmospheric optics, light scattering, state-specific chemical reactions and radiative signatures of missile plumes, and sensor out-of-field-of-view rejection.